A&A 411, L153–L157 (2003)
DOI: 10.1051/0004-6361:20031259

Astronomy & Astrophysics

IBIS Veto System⋆

Background rejection, instrument dead time and zoning performance

E. M. Quadrini[1], A. Bazzano[1], A. J. Bird[2], K. Broenstad[3], F. Di Marco[4], G. La Rosa[1], M. Michalska[5], P. Orleanski[5], A. Solberg[3], and P. Ubertini[1]

[1] Istituto di Astrofisica Spaziale e Fisica Cosmica, Italy
[2] Departement of Physics and Astronomy, Southampton University, Southampton, UK
[3] Universitet I Bergen, Fysisk Institutt, Bergen, Norway
[4] VEGA IT GmbH c/o European Space Operation Centre-ESA, Darmstadt Germany
[5] Centrum Bada Kosmicznych PAN (PAS-SRC), Warszava, Poland

Received 14 July 2003 / Accepted 8 August 2003

Abstract. IBIS is the high energy imager on board the INTEGRAL satellite. The gamma-ray instruments on board will take advantage of the long uninterrupted observation made possible by the very eccentric orbit (10 000 km perigee and 152 000 km apogee). A disadvantage for orbits outside the protection of the van Allen belts is the exposure to cosmic and solar particles. Conversely, the background is quite stable throughout the 3 days orbit. In order to maximise the scientific returns and take full use of these almost 3 days continuous observations, IBIS is equipped with a light, very effective Veto System. This ensures a substantial reduction of the background due to the induced photon and hadronic component, in turn enhancing the detector sensitivity. The performance of the IBIS veto as evaluated during telescope commissioning is reviewed. In particular, the efficiency of background rejection and the resulting IBIS dead time are evaluated as well as the impact of different zoning configurations. Measured over the whole energy range, the veto system provides a background suppression effect of ~50% for ISGRI and ~40% for PICsIT. The definitive veto settings optimised for the operational working temperature and background conditions are described.

Key words. INTEGRAL – gamma-ray – veto – calibration

1. Introduction – The IBIS veto system

The IBIS veto system design and the results of laboratory tests have been described previously in papers Ubertini et al. (1996), Bazzano et al. (2003), Poulsen et al. (2000) and in technical documents IBIS User Manual (vol. 1), IBIS User Manual (vol. 2), IBIS FM VETO Calibrations (2001). The IBIS shielding system design derives from the challenging limited resource allocations in terms of weight and power. These led to the limitation of the active lateral shield height up to the bottom of ISGRI (the lower energy detector layer), to design the active Veto Detector Modules (VDMs) in four different shapes for shield leakage minimisation, and to use a passive shield between the mask and the detector. There are 8 lateral and 8 bottom VDMs.

Fig. 1. Rear veto assembly.

The bottom array and four lateral modules can be seen with their main components in Figs. 1 and 2. Each module comprises two BGO scintillation crystals optically glued along their long edge. The composite crystal is viewed by two PMTs with embedded Front End Electronics (FEA) and high voltage (HV) divider. Cross bars stiffen the two electronic units, i.e. Veto

Send offprint requests to: E. M. Quadrini,
e-mail: mauro@mi.iasf.cnr.it

⋆ Based on observations with INTEGRAL, an ESA project with instruments and science data centre funded by ESA member states (especially the PI countries: Denmark, France, Germany, Italy, Switzerland, Spain), Czech Republic, Poland, Norway and UK, and with the participation of Russia and the USA.

Table 1. 511 keV line fit parameters for VDMs before and after final setting.

VDM	Initial settings			After tuning		
	Peak (chan)	σ (chan)	*FWHM* (%)	Peak (chan)	σ (chan)	*FWHM* (%)
1	50.7	4.66	21.7	25.8	2.9	26.6
2	50.3	6.7	31.3	26.6	3.3	29.4
3	53.5	5.3	23.4	27.7	4.0	34.4
4	50.8	5.2	24.2	26.7	3.2	28.5
5	50.7	6.3	29.2	25.6	3.2	30.2
6	46.3	6.1	31.3	25.2	3.5	32.9
7	47.5	7.1	35.0	26.4	4.9	43.4
8	51.7	6.5	29.8	26.7	3.3	28.6
9	51.7	4.4	20.1	26.5	2.7	24.8
10	49.0	4.7	22.6	26.0	2.9	26.6
11	–	–	–	27.4	4.0	35.0
12	55.9	5.5	23.2	25.8	3.4	31.0
13	49.9	4.5	21.1	26.4	2.8	25.2
14	53.6	5.9	25.9	24.4	2.7	22.8
15	50.6	5.5	25.4	25.0	3.4	31.7
16	50.5	4.9	23.1	26.6	2.9	25.4
Total	50.9	5.8	26.5	26.3	2.9	25.9

Fig. 2. IBIS showing lateral and rear veto.

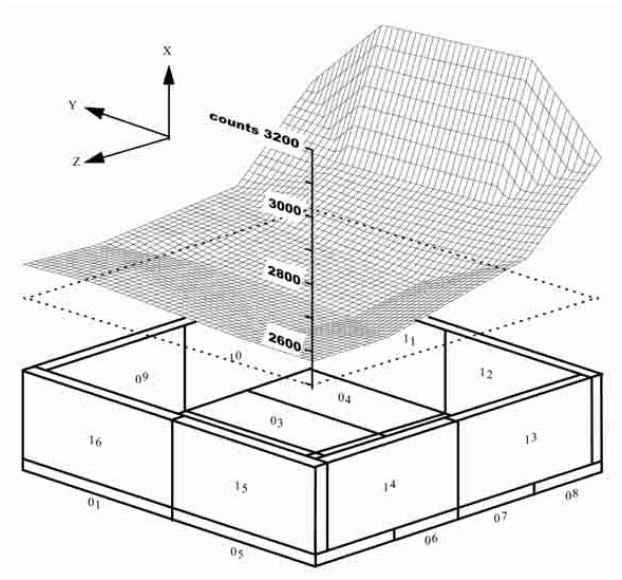

Fig. 3. Background count distribution.

Module Electronics (VME) for control and signal conditioning and High Voltage Power Supply (HVPS). In each module the HVPS is distributed to the two PMTs whose signals, adjusted through two VME independent gain chains, are summed. The sum is delivered to the Veto Electronics Box (VEB) where all signals are discriminated, converted into strobes with adjustable length and delay, and distributed to the two detector layers ISGRI and PICsIT. The VEB also provides for module control and housekeeping (HK) data collection. Here, each HV, gain, discrimination level, strobe delay and width can be independently programmed. The strobes can also be grouped according to the proper zoning' configurations making the system very flexible and adaptable to different environmental conditions. Parameter optimisation and calibration are facilitated by collection of 256 channel VDM spectra from either a single selected VDM or from each VDM in sequence. Spectra may be acquired in coincidence or not with the On-Board Calibration Unit (OBCU) strobes.

2. Module equalisation

At the end of the first activation phase, the veto modules were equalised through the set of parameters selected during the Parameter Optimisation and calibration campaigns Bazzano et al. (2003), Poulsen et al. (2000), IBIS FM VETO Calibrations (2001).

A set of spectra were collected in coincidence with the Calibration Unit which provides a clear line of 511 keV photons. Table 1 lists the parameters of the 511 keV line fits: peak position, energy resolution and standard deviation. Finally, there is the mean for all 16 modules. The energy resolution value is affected by threshold effects in the 8-bit ADC channels, enhanced by the resultant poor statistics due to the short integration time. At this stage, VDM 11 was operated with a low

Table 2. Veto strobe generation tests.

Active module	ISGRI zoning	PICsIT zoning	ISGRI/PICSIT strobe ratio
Mod 1 and 16	all	all	4.0
Mod 1 and 16	lateral	all	4.9
One at a time	lateral	all	4.0

HV (1.0 kV) set after problems that occurred during Thermal-Vacuum test in ESTEC.

Figure 3 shows the veto background count rates taken from each individual VDM. The figure shows the shape of the veto system background response, based on an irregular grid defined by the centre of each VDM BGO block and interpolated (average) values at the corners. The plot shows that the modules closest to the other instruments and the main spacecraft structures ($-Z$ direction) have higher counts than the modules farthest away. This is due to secondary background production, the closeness to this source region located towards the centre of the spacecraft, and the greater solid angles for these VDMs with respect to the source region. The regularity shown indicates a successful calibration and setup of the veto system.

A number of tests were performed (Table 2) to compare the veto strobe counts for different ISGRI zoning configurations. For both ISGRI and PICsIT, *veto all* indicates that the detectors receive a logic OR signal from all lateral and bottom veto elements. Conversely, when ISGRI zoning is set to *lateral*, the ISGRI strobe derives from the logic OR of just the lateral VDMs. On this basis, counts from a single module can be meaningfully compared to the combination of VDM 1 and 16 (one rear, one lateral).

The expected ratio between ISGRI and PICsIT veto strobe counters is 4.0 due to a division factor applied to the PICsIT counter. Nevertheless, the sum of bottom and lateral VDM counts are about 20% more than total veto counts coming from the "lateral.OR.bottom" strobes. This provides a raw estimate of the cosmic particle contribution to the background. In fact, most of the particles, because of their energy, interact with two or more VDMs leading to a single strobe when the *veto all* configuration is applied. False coincidences contribute only about 4% of this difference. Corresponding multiple-site fractions on ground were 4% at Laben (of a total ~9300 c/s) and 2.5% at ESTEC (of a total ~3700 c/s).

3. Temperature dependence

The veto first activation was performed in three main steps after an outgassing period of 15 days. First step was a check on two Modules (1 and 16) and on the two Calibration Units. The latter are the most critical being positioned on the tube wall far away from all other heat sources. Finally, all modules were checked one by one during one day test and then the whole system was activated.

Figure 4 shows that all module temperatures are between the warmer VDM4 and the colder VDM13 in a range of ~8 °C. CDM1 and 2 values are given for reference only. Figure 5 is a 3D representation of the spatial temperature distribution 12 hours after the activation.

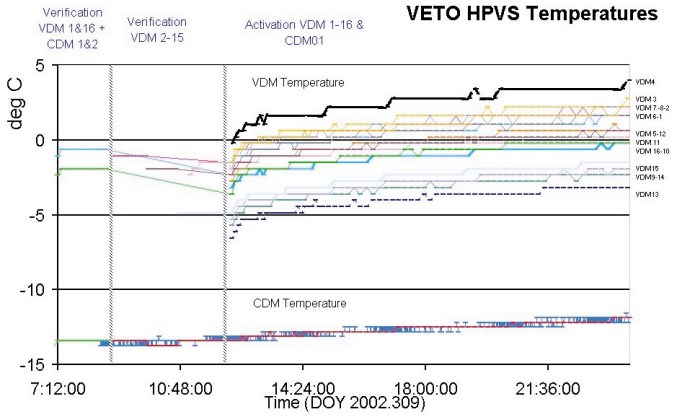

Fig. 4. VDM temperatures after first activation.

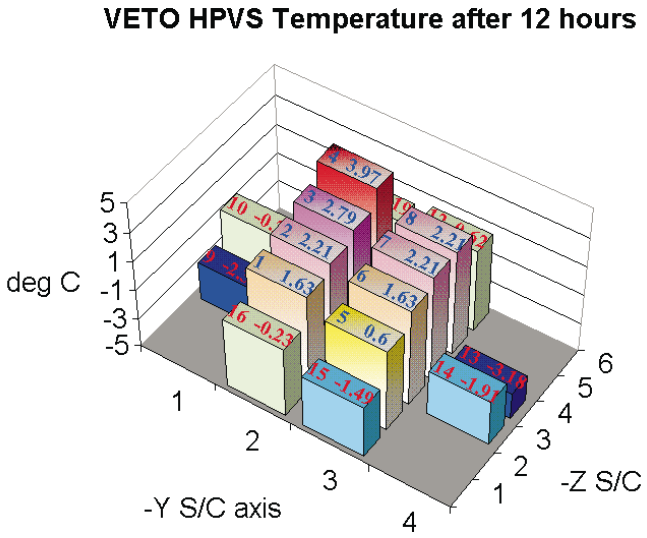

Fig. 5. Veto spatial temperature distribution after 12 hours.

The gradient between the veto modules is explained in terms of distance from different heating sources, position with respect to INTEGRAL axis, heaters or cooling straps, thermal exchange with other sub-systems, effect of sun aspect angle. It is also simple to observe the module differential heating following booster heater activation. What is important to stress is that each module has good thermal stability and the temperature difference between modules is constant along the orbit.

The thermal behaviour in different operational conditions is also important. The temperature variation during Perigee with and without Eclipse was assessed during commissioning. The veto is always off during the radiation belt passage for safety (i.e. below 60 000 km from the Earth). The not-operative temperature is as usual controlled by the INTEGRAL thermal control loop. The average variation in the Eclipse season is ~1 °C/hr for the VDMs. The strobe count rate is not appreciably affected by this variation (Fig. 6).

When not in the Eclipse season, the VDM HVs are off for about 7 hrs during the perigee passage. In this case, with most of the Instrument on, the modules reach minimum values ranging between −12 and −2 °C and the booster heaters are not activated. The plateau temperature is then recovered after

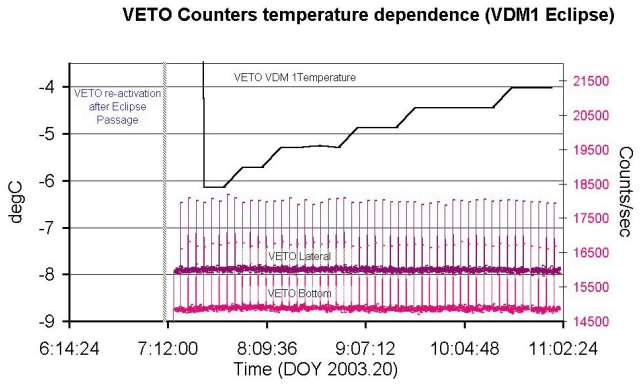

Fig. 6. Temperature evolution after perigee; with eclipse.

the new switch on at 0.3 °C/hr, while the single module temperature variations during the orbit are within 3 °C. It is worth to note that the Veto System gain and strobe count rate stability comes directly from this good thermal behaviour along the whole orbit in all conditions.

4. Veto zoning and efficiency

There are two criteria on which the veto efficiency can be judged.

The first of these, reduction in count rate, i.e. detector background, is a crude measurement of the veto efficiency since it does not consider whether the reduction in count rate is at the expense of a poorer signal-to-noise ratio, or is being achieved, for example, just by increasing the detector dead time.

For the veto to induce an improvement in signal-to-noise, it must be seen to be preferentially removing background events and thus be performing at a better level than a simple grey filter. In the case of the zoning modes for ISGRI and PICsIT vetoing, it is this criterion which is appropriate. When making assessment of veto performance using in-flight data, it is crucial that dead-time corrections are made so that the improvement over a grey filter can be established. In the following analysis we refer to veto configuration and data collected during commissioning on 11th Nov. 2002.

The effect of each zoning mode can be assessed by comparing the reduction in count rate compared to the *no veto* case with the reduction in count rate due to extra dead time alone. Any additional reduction indicates an increase in vetoing effect that should translate to an improvement in sensitivity, provided that there is a real effect of vetoing on background and a negligible effect on the source to be observed.

Thus we can conclude that for ISGRI, the vetoing effect probably increases marginally from *lateral* to *veto all* modes,

Table 3. ISGRI veto efficiency.

Config	Before[1]	After	Change	Dead Time[2]	Veto Effect
No veto	2500	2500	0%	0%	0%
Zone Lat	2500	1146	54%	8.7%	45%
Zone All[3]	2500	750	70%	14%	55%
Zone All[4]	2500	880	65%	14%	51%

Table 4. PICSIT veto efficiency

Config	Before	After	Change	Dead Time	Veto Effect
No veto	4850	4850	0%	0%	0%
Zone C	4850	3400	30%	1.8%	28.2%
Zone D	4850	3100	36%	2.4%	33.6%
Zone All	4850	2750	43%	4.2%	39%

although the reduction in count rate is certainly largely due to the increased dead time from the increased number of veto strobes. In theory, the errors in the determination of the *no veto* rate would require further analysis of this problem. In practice, the pressure on telemetry space means that the use of *veto all* zoning is most appropriate since it is at worst acting as a grey filter in comparison to *lateral*, but in all probability is further improving the signal to noise for ISGRI events.

The assessment for PICsIT data is somewhat different due to the use of histograms which avoid issues of telemetry saturation, thus the *no veto* rate can be simply measured from telemetered science data. Therefore the rates are more securely defined for the PICsIT case.

However, the use of zoned veto signals, which act on only a fraction of the detector plane, modify the dead-time calculation somewhat, and it is simplest to determine the dead time, on a per-module basis, from the PICsIT detector module strobe counters. Again, calculating the background reduction on PICsIT data, assuming a PICsIT-VETO strobe length of 2 μs, yields:

Again the conclusion is that the vetoing efficiency increases as more of the detector plane receives the veto strobe (i.e. as zoning is reduced), and that *veto all* is the optimum zoning configuration for PICsIT.

5. Final setting

During the commissioning phase, the veto system exhibited nominal behaviour apart from two unexpected features: three times one VDM HV dropped to zero and occasional high count rates (>50 000 c/s) were observed in single modules lasting from one to several hours.

These phenomena were difficult to explain due to their random occurence, and they could not be reproduced on the QM on the ground. One possible explanation was the presence of frozen water vapour or other volatiles due to CFRP degassing during the initial part of the flight. Another was HV instability induced by occasional very high energy particles. A deep

[1] Obtained from unsaturated sections of telemetry. This throughput is not sustainable with actual TLM and the determination has large errors.

[2] Dead time assumes 6 μs ISGRI-VETO strobe length which was in use during these tests.

[3] This will give an over-estimate of the veto effect since there will be more Compton events generated due to the high rates in PICSIT.

[4] Includes the effect of Compton events in the previous case to give a better comparison to the no veto case.

[5] After optimisation at −6 °C.

Table 5. PICsIT veto final settings.

VDM	V01	V02	V03	V04	V05	V06	V07	V08
Activation HV[5]	1178	1202	1240	1186	1169	1193	1247	1207
Present HV	1002	1022	1034	989	1001	1014	1099	1002
PMT gain ratio	0.29	0.29	0.25	0.25	0.30	0.29	0.38	0.24
VME pre amp ratio	1.73	1.73	2.00	2.00	1.64	1.73	1.32	2.08
VDM	V09	V10	V11	V12	V13	V14	V15	V16
Activation HV	1156	1154	1276	1149	1203	1143	1094	1147
Present HV	1001	1038	1064	1005	1003	1005	999	1001
PMT gain ratio	0.33	0.44	0.25	0.35	0.25	0.38	0.5	0.35
VME pre amp ratio	1.50	1.13	2.00	1.42	2.00	1.33	1.00	1.42

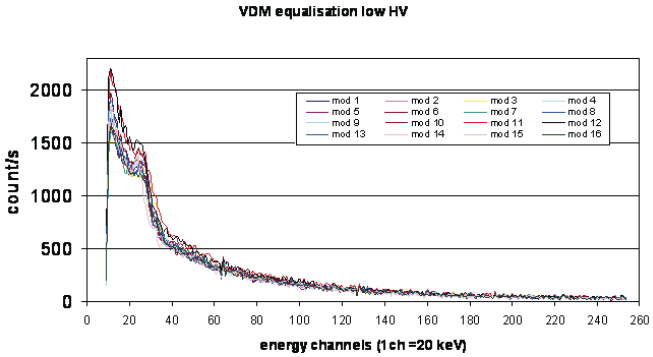

Fig. 7. Spectra for final configuration.

investigation was performed to improve the long-term stability of the veto system. and it was decided to reduce the PMTs HV power supply to the minimum value, to increase the electronics pre-amplifier gain to 2 keV/mV to compensate for the loss of gain in the PMTs, and to set the electronic threshold to 40 mV (in Table 5). In this way the design goal of 80 keV energy threshold was maintained.

A series of VDM spectra were recorded in the final configuration, and are shown in Fig. 7. The fit parameters obtained for the 511 keV lines in those spectra are reported in Table 1.

The veto system has performed stably since these settings were adopted, and the fact that there is no degradation in the measured energy resolution indicates that the veto detectors themselves are still performing well.

6. Conclusions

The effectiveness of the veto design has been confirmed during the Commissioning Phase by a background suppression of 50% for ISGRI and 40% for PICsIT, while inducing an acceptable dead time (<15% for ISGRI and 4% for PICsIT. This results is a good agreement between the recorded detector rates and early project assumptions.

The flexibility of the system was used to reach stable working conditions in the flight environment without compromise on instrument characteristics. To date, the system shows a good thermal and performance stability, with all modules working in nominal conditions throughout the orbit, including the eclipse sessions.

Acknowledgements. The authors would like to thank the Laben team for the veto engineering, S. Di Cosimo and U. Zannoni for their important support; A. Segreto and M. Gabriele for data collection facilities. The Italian part of IBIS is funded by the Italian Space Agency, ASI. The Norwegian part of IBIS is funded by the Research Council, NRC. The polish participation was founded by State Committee of Scientific Research of Poland. A. J. Bird is funded by PPARC grant GR/2002/00446.

References

Bazzano A., Bird A. J., Laurent P., et al. 2003, Proc. PSD6, September 9th–13th 2002. Accepted for publication in NIM.

IBIS Team, IBIS User Manual 5.1, vol. 1, EID-B. IN.IB.IAS.UM.010/01

IBIS Team, IBIS User Manual 5.1, vol. 2, Veto user manual. IN.IB.IAS.UM.010/01

IBIS Team, Report on IBIS FM VETO Calibrations, Dec. 2001, IN.IB.IAS.RP.026/2001

Poulsen J. M., Sarra P. F., Hajdas W., et al. 2000, SPIE, 4140, 293

Ubertini P., Di Cocco G., Lebrun F., et al. 1996, SPIE 5-7, 2806, 246